Materials Research Proceedings **27** (2023) 173-182 https://doi.org/10.21741/9781644902455-22

Investigation of vibrational assessment on osseointegration process with a novel implant design

Shouxun Lu[1, a *], Benjamin Steven Vien[1, b], Matthias Russ[2, 3, c], Mark Fitzgerald[2, 3, d] and Wing Kong Chiu[1, e]

[1]Department of Mechanical & Aerospace Engineering, Monash University, Wellington Rd, Clayton Vic 3800, Australia

[2]The Alfred Hospital, 55 Commercial Road, Melbourne Vic 3004, Australia

[3]National Trauma Research Institute, 89 Commercial Road, Melbourne Vic 3004, Australia

[a]shouxun.lu@monash.edu, [b]ben.vien@monash.edu, [c]M.Russ@alfred.org.au, [d]M.Fitzgerald@alfred.org.au, [e]wing.kong.chiu@monash.edu

Keywords: Osseointegration Process, Vibrational Analysis, Structural Health Monitoring

Abstract. Osseointegrated prosthesis has been utilized as an alternative treatment for transfemoral amputation to replace the common prosthetic sock device, which has been complained by patients as unsatisfactory due to the severe infection and pain. Osseointegrated prosthesis demonstrated enormous advantages in improving mobility and quality of life for the amputee. However, the long rehabilitation period, which forces patients to stay in bed for up to 18 months, limits the application of the osseointegrated implant. Therefore, accurate and quantitative assessment method attracts research interest in recent years. This paper investigates the capability of a vibrational analysis technique using two unidirectional sensors on monitoring stages of the osseointegration process. This assessment method has been proven to be sensitive to the stiffness change at the femur-implant interface due to osseointegration. This paper mainly focuses on the further validation of this vibrational method and E-index on three lengths of the residual femur. The colormap of the cross-spectrum against the curing time demonstrates a clear step change in the magnitude. Moreover, the E-index for these three lengths of residual femur shares a similar trend, which dramatically increases after 300s and peaks above 0.8. The time when the gradient of the E-index reaches its maximum is coincident with the initial bonding time of the epoxy adhesive which is used to simulate the osseointegration process. The clear correlation between E-index to the curing time evidences the capability of this vibrational method in monitoring the osseointegration process and the potential of the E-index being a quantitative parameter to assess the stage of the osseointegration process.

Introduction

Traumatic limb loss affects over 50 million patients worldwide [1]. Prosthetic limbs offer a relatively secure and comfortable connection to the residual limb, improving the life quality of amputees. The traditional design of the prosthesis is using the socket interface which contains a socket that covers the remnant femur and links with the artificial limb, leading to severe skin infections and pain in long-term utilization [2, 3]. Moreover, the application of the socket system is limited by the specific requirement for the length of the residual limb [2, 4, 5]. The trans-femoral osseointegrated implant (TFOI) is treated as an alternative method for amputees who suffer from an above-knee amputation [3]. Unlike a conventional socket system, the osseointegrated implant provides a direct connection between the residual limb and prosthesis by inserting the intramedullary stem into the skeletal system. There are several types of TFOI currently clinically available, such as the OPRA system and the ILP system. Patients with the osseointegrated implant

experience significant improvement in control of prosthesis and joint mobility over the socket system [6-8].

Even though the OI system has significantly reduced and eliminated some limitations of the socket system [3, 7-10], various challenges remain for the osseointegrated implant, such as infection and implant failure. It has been evidenced that there are approximately 40% of patients suffered from infection, which mainly due to penetration of the implant [11]. Except for these limitations, an extensive long rehabilitation period has also become another major concern for the osseointegration implant. During the rehabilitation period, bone formation starts on the surface of biocompatible material without the intervention of inter-positioned connective tissue [9, 12, 13]. The improved stability of the implant due to the stiffness increase at the femur-implant interface is associated with the osseointegration process. Loading on the implant is restricted during the rehabilitation, to avoid overloading at the femur-implant interface. In addition, this also prevents the host bone damage and implant loosening. However, the slowness of the this inevitable period causes amputee's concern and frustration [14]. Hence, reliable assessment methods for the OI process are essential to ensure initial and long-term implant stability. Currently, various examination methods such as clinical X-ray and magnetic resonance imaging are used to assess the in-vivo implant stability [3, 15, 16]. Nonetheless, these conventional methods are known to be subjective and qualitative since their accuracies are mainly based on the interpretation and judgment of the surgeon rather than using quantitative justifications (i.e. stiffness of the connection) [2, 16-19]. Therefore, there is a significant interest in researching the robust and quantitative method on monitoring the osseointegration process to personalise the rehabilitation period based on the patient's conditions.

Mechanical vibrational analysis is a non-destructive technique, which was widely used in the assessment of the dental implant stability [15, 17, 20], monitoring the total hip arthroplasty loosening [3, 21-25]. The research of vibrational methods on assessing the degree of osseointegration for transfemoral implants has proven that the change in the dynamic properties of the bone-implant system, such as resonance frequency and vibration modes, could identify the variation of bone-implant interface conditions along with osseointegration progression [3, 15, 26-28]. In the in vivo research reported by Shao et al [3], the resonance frequency gradually increased during the rehabilitation process of a 40-year-old male patient, except for a reduction at first weight bearing. Moreover, Cairns et al [15, 16] investigated the sensitivity of resonance frequency and mode shape to the change at the femur-implant interface by varying the implant inserting torque. The result demonstrated that by tracking the change in the particular modes over a specific frequency range, it is possible to identify the degree of osseointegration. Recently, research conducted by Lu et al [29] showed that the progression of the simulated osseointegration process could be identified by utilising a time-progression cross-spectrum with a dual sensor measurement method. In addition, they also proposed a new vibration parameter energy index (E-index), which focused on the magnitude over a large frequency range from 0 to 10kHz, instead of selecting and identifying the resonance frequencies based on the implant shape and residual femur length. The results in the previous study revealed that E-index was significantly sensitive to the stiffness change at the femur-implant interface regardless of the femur cross-section. In this paper, This paper mainly focuses on the further validation of this vibrational method and E-index on three lengths of the residual femur under in vitro conditions.

Methodology

The femur models which represented three different osteotomy levels of 228 mm, 190 mm and 152 mm measured from the knee respectively, were utilised in the experiment (see Fig. 1a). The finding in [29] illustrated that the change in the cross-section of the residual femur has limited effect on the accuracy of the vibrational method investigated in this study. Therefore, the primary parameter that is of interest was the residual length and not the cross-section shape of the implant.

Materials Research Proceedings **27** (2023) 173-182 https://doi.org/10.21741/9781644902455-22

Hence, in this study only an oval-shape implant was employed in this experiment to maintain the consistency between each femur specimen. The implant design utilised in this study was developed according to a design concept proposed by Russ, Fitzgerald, and Chiu (US20200188140) [30, 31], which aims to embed sensors into the implant to assess implant stability under in vivo conditions. The geometry of the custom-fit implant, shown in Fig. 1b, consisted of three components: cup-shaped extramedullary (EM) strut, an intramedullary (IM) stem and a prosthesis stem. EM strut provided the initial resistance to the axial and rotational movement, allowing close apposition of bone to the surface of IM. After forming a secure connection between femur and implant, the weight bearing load was applied thought the abutment, which was connected to the prosthesis stem.

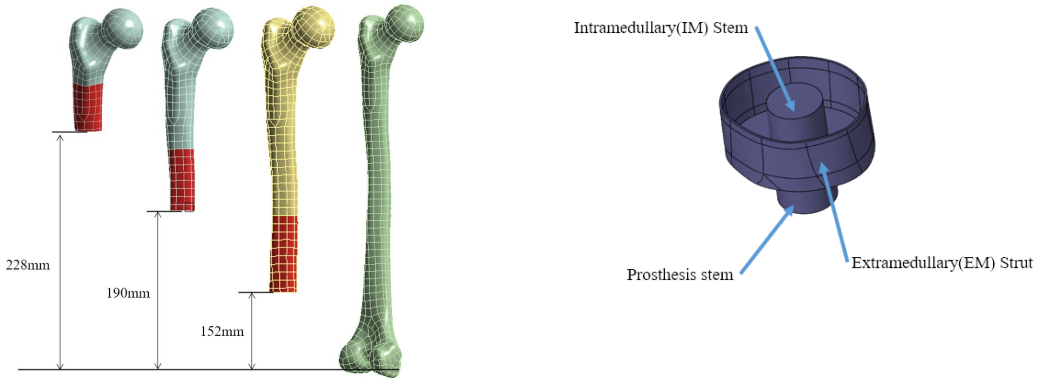

(a) **(b)**

Fig. 1. Geometry of (a) Three lengths of residual femur compared to the intact femur(Green) and (b) The novel osseointegration implant developed based on Patent US20200188140.

The implant specimens were 3D printed with ABS. The stem was extended from the base to provide a loading point for the experiment. The diameter of the IM stem was slightly reduced by 2 mm to provide sufficient space for the application of the epoxy adhesive, which was used to simulate the osseointegration process for the in vivo implant [2], as shown in Fig. 2b. An epoxy adhesive with a setting time of 5 mins and a fully cured time of 16 h was used. Even though the material properties of the adhesive are not an accurate representation of the osseointegration process, the change in stiffness as a result of the curing process is similar to the bonding between femur and femur introduced by the osseointegation process [18, 19, 32-35].

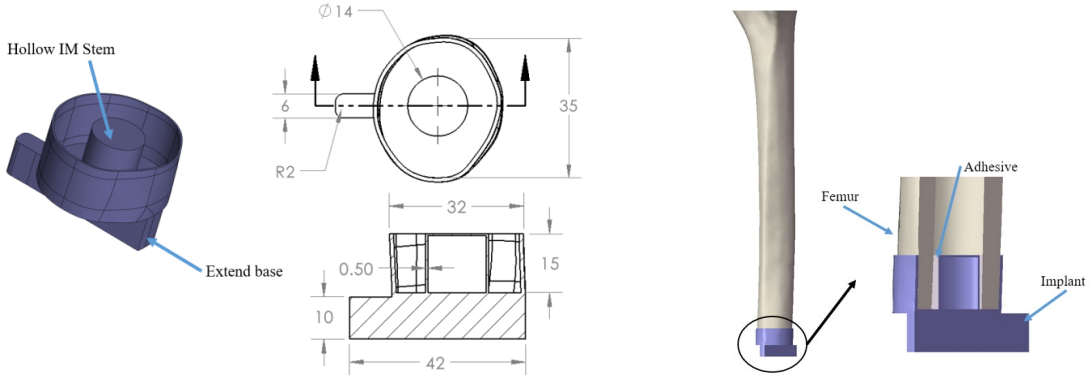

(a) **(b)**

Fig. 2. (a) Modified oval-shape implant with hollow IM stem for the experiment and (b) Cross-section of femur-implant interface with adhesive epoxy

Materials Research Proceedings **27** (2023) 173-182 https://doi.org/10.21741/9781644902455-22

In the experiment, a 250 mm long Sawbone® composite femur model was fastened rigidly by a vice through 3D printed adapter, as illustrated in Fig. 3. The femur mode was clamped at different sections to simulate three length conditions of residual femur. The femur-implant system was stimulated by an input loading through the strike point with an instrumented impact hammer (B&K Type 8206). Two unidirectional accelerometers (B&K Type 4507), which were attached to the bottom of the implant at location of S1 and S2, were arranged to measure the acceleration along y-axis. The voltage from two sensors were acquired and analyzed by B&K PULSE with a frequency bandwidth of 14.4kHz and frequency resolution of 1.125Hz. Due to the significant increase in stiffness of the adhesive in the first 5 mins, the data were recorded at 30-second intervals for the first 5 mins and 60-second intervals for 14 mins.

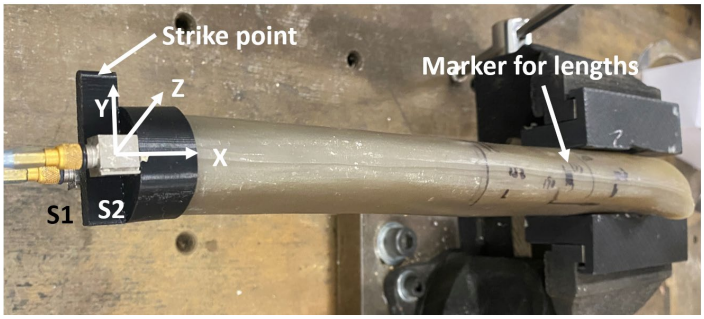

Fig. 3. Two-sensor setup for composite femur model with markers for three residual length conditions.

The quality of the recorded signals and acceptable frequency range were evaluated and determined via a coherence function as illustrated below:

$$Coherece = \frac{\left|\overline{G_{11}(f)}G_{22}(f)\right|^2}{G_{11}(f)G_{22}(f)} \tag{1}$$

where $G_{11}(f)$ and $G_{22}(f)$ are the autospectra of sensors 1 and 2, respectively, and $\overline{G_{11}(f)}$ is the complex conjugate of $G_{11}(f)$.

The E-index from the previous study was defined as ratio of integration of normalised magnitude plot from a certain frequency range from lower frequency bound f_0 to target frequency f_i relative to the whole frequency range (f_0 to f_1), refer below [29]:

$$E(t) = E_{fi}(t)/E_{total}(t) \tag{2}$$

$$E_{f_i}(t) = \int_{f_0}^{f_i} M^2(f,t)df \tag{3}$$

$$E_{total}(t) = \int_{f_0}^{f_1} M^2(f,t)df \tag{4}$$

where $M(f,t)$ is the normalized magnitude at frequency f and cure time t, $E_{total}(t)$ is the integration of normalised magnitude $M(f,t)$ from f_0 to f_1 at cure time t, E_{f_i} is the integration of normalised magnitude $M(f,t)$ from f_0 to f_i at cure time t.

The selection of f_0, f_i and f_1 varies between each residual length condition and will be discussed in the result section.

Materials Research Proceedings **27** (2023) 173-182 https://doi.org/10.21741/9781644902455-22

Result

Determination of upper frequency band

The coherence, which was plotted against the adhesive cure time in frequency bandwidth of 14.4kHz for three residual length conditions was shown in Fig. 4. For all three conditions, the magnitude distributed over a wide frequency range without significant peaks before 300s. However after 300s, marked with yellow dashed line, several resonance peaks could be identified at certain frequencies. These results indicated that resonance modes were suppressed by the damping effect of the adhesive prior to the sufficient strength at the femur-implant interface. Moreover, the plots illustrated that the coherence from 0 to 8000Hz, were generally above 0.8 indicating that the veracity of the data collected. Therefore, the upper bond (f_1) in Equation (4) was set to 8000Hz.

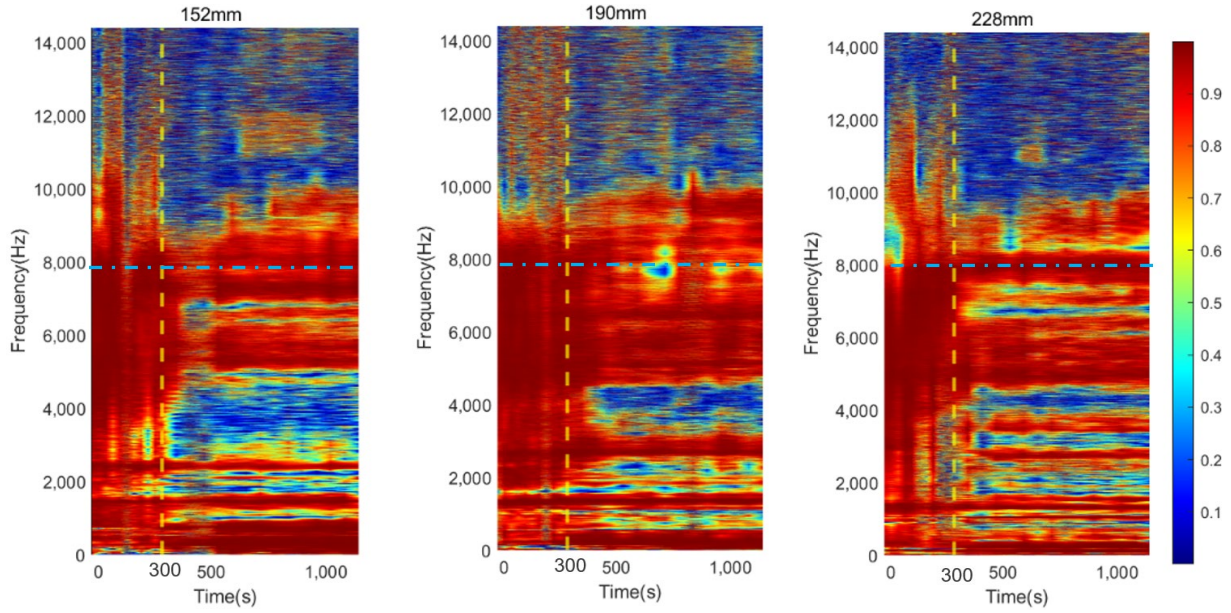

(a) **(b)** **(c)**

Fig. 4. Coherence function for residual length of (a) 152 mm, (b) 190 mm and (c) 228 mm.

Time-progression of Cross-spectrum

Fig. 5 exhibited the cross-spectrum of the normalized magnitude, which were plotted in the frequency bandwidth of 8000Hz for three residual femur lengths. The cross-spectrums were plotted at a cure time of 0, 150, 300, 600, and 1140 seconds, which aimed to show the magnitude change relative to the simulated osseointegration process. For all three length conditions, at the early stage of the adhesive curing process (before 300 seconds), the response was flat and the resonant modes were hard to spot in the plots except for the vibration modes located at the lower frequency range (frequency smaller than 1500Hz), as marked with vertical dash-dotted line. There are several peaks that could be visually recognized in the cross-spectrum after the adhesive setting time of 300 seconds such as 2500, 2900, 2700Hz for 152, 190 and 228 mm respectively, as indicated in the plot. Along with a cure time increasing, the selected peak became noticeable with curing time. This finding indicated that the change of the interface condition could be detected by the specific resonant modes by track the change along the curing time.

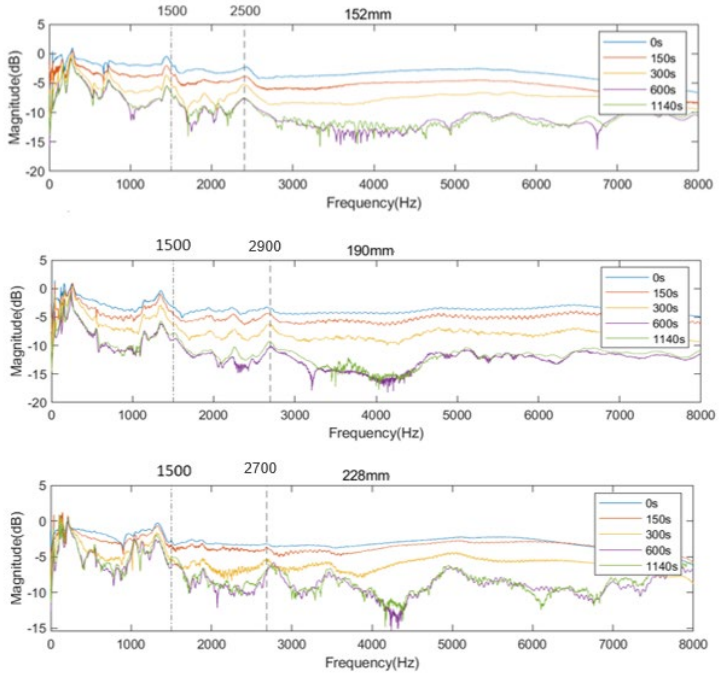

Fig. 5. Cross-spectrum of normalised magnitude for three residual femur length at cure time 0, 150, 300, 600, and 1140 seconds.

Different from Fig. 5, the colormap in Fig. 6 demonstrated the development of the resonance peaks over a continuous time frame rather than several discrete time spots. Before 300 seconds, which was indicated with a vertical yellow dash-dotted line, the vibration modes were hard to determine except for the modes that located below 1500Hz, which were not affected by the interface condition change. Therefore, the lower frequency bound for the E-index, f_0 was set to 1500Hz for all three length conditions, refer to Equation (3) & (4). By setting the lower bond of integration, the ability of the E-index on monitoring the degree of osseointegration was enhanced by excluding the frequency peaks not being relevant to the simulated osseointegration process. During the early stage of curing time, the frequency modes over 1500Hz are impeded by the damping induced by the soft adhesive. A clear step change on the magnitude of resonance peaks at 300s, which is coincident with setting time. After 300s (5 mins setting time), multiple resonance peaks appeared, especially for the peaks located between 2000 to 3000Hz. With the further curing of the adhesive, large variation in the resonant peaks along the cure time were identified around 2500Hz for 152 mm , 2900Hz for 190m and 2700Hz for 228 mm conditions. Therefore, to enhance the sensitive of the E-index, the target frequency f_i was set to 2500, 2900 and 2700Hz for 152, 190 and 228 mm, respectively, refer to Equation (3), to ensure that frequency range covered by the E-index has large magnitude changes related to the stiffness changes induced by the simulated osseointegration process.

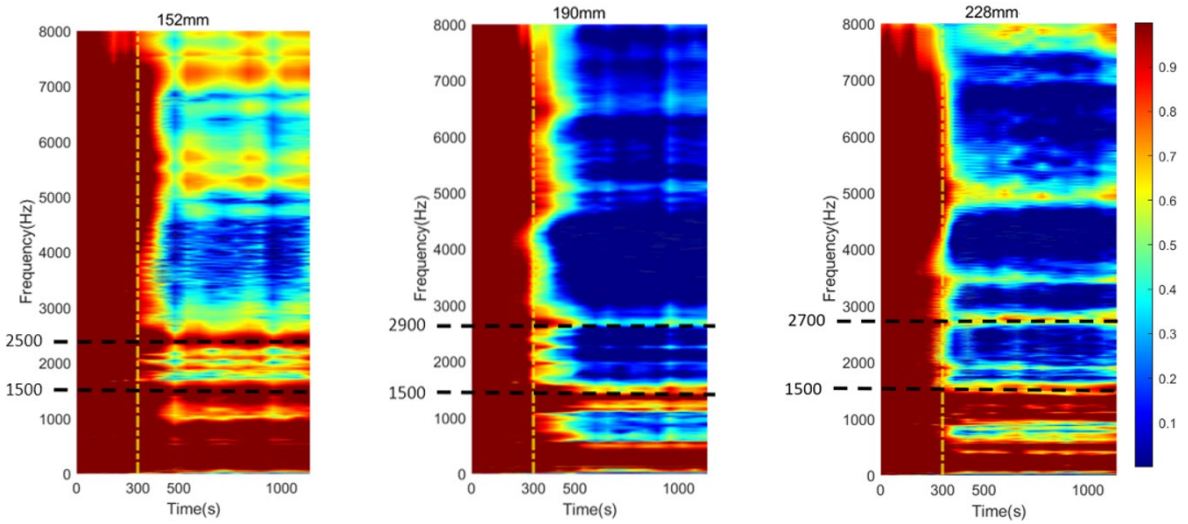

(a) **(b)** **(c)**

Fig. 6. Time-progression of cross-spectrum as the function of cure time for (a) 152 mm, (b) 190 mm and (c) 228 mm

E-index as function of curing time

Fig. 7 generated from the E-index formula based on the specific frequency ranges selected based on the above results for each remnant femur length. Even though there are some fluctuations in the E-index, the plots share a general trend that the E-index gradually increases to a value and stabilises above above 0.8, indicating the implant securely bonded with the femur. This behaviour of E-index over curing time evidenced that the interface stiffness change incurred by the curing of the adhesive is clearly represented by the the E-index through time. In addition, Table 1 demonstrates the change in the E-index at the end of the experiment relative to the value at t = 0. The E-index demonstrated an averaged increase over 50% with minimum change of 47%, which is significantly larger, compared to the 3% of resonance frequency analysis [3] and 10-47% difference and modal analysis [15], for all three remnant length conditions.

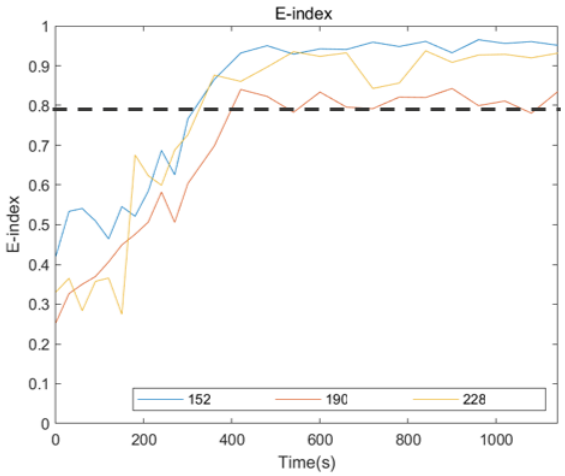

Fig. 7. E-index development as the function of cure time.

Table 1 Difference of E-index (Relative to the 0s) for each length condition

Length	Difference (relative to t_0) (%)
152 mm	52.55
190 mm	47.59
228 mm	54.89
Averaged	**51.67**

Conclusion

The work presented has shown that the degree of the osseointegration which is simulated by using two-part adhesive epoxy, could be assessed with the dynamic response of femur-implant system. Cross-spectrum and colormap of the normalised magnitude over curing time, has demonstrated significant changes which were related to the increase in stiffness due to the curing of epoxy, indicating that the application of these plots could advance the accuracy of diagnostic techniques. Furthermore, the accuracy and reliability E-index from previous work [29] is further investigated in this study with three residual femur length conditions. The results have indicated a clear trend and significant shift of averaged 51% of E-index along the simulated osseointegration for all three lengths. This finding evidenced the capability of E-index as a quantitative approach to monitor the degree of osseointegration without the burdens of selecting and identifying the specific resonant peaks based on length of residual femur. Future work includes the validation of this E-index method, and research on combining the E-index method with the novel implant, which will intergrate the sensors with structure to assess the osseointegration under in-vivo conditions.

Funding:
This research is funded by the US Navy Office of Naval Research (N62909–19–1–2051). The financial support provided by the Office of Naval Research is gratefully acknowledged.

Conflict of Interest
The author declares that there is no conflict of interest regarding the publication of this paper.

Ethical approval
This article does not contain any studies with human participants or animals performed by any of the authors.

References

[1] McDonald, C.L., et al., *Global prevalence of traumatic non-fatal limb amputation.* Prosthetics and orthotics international, 2021: p. 0309364620972258.
[2] Wang, W. and J.P. Lynch, *IWSHM 2017: Application of guided wave methods to quantitatively assess healing in osseointegrated prostheses.* Structural Health Monitoring, 2018. **17**(6): p. 1377-1392. https://doi.org/10.1177/1475921718782399
[3] Shao, F., et al., *Natural frequency analysis of osseointegration for trans-femoral implant.* Annals of Biomedical Engineering, 2007. **35**(5): p. 817-24. https://doi.org/10.1007/s10439-007-9276-z
[4] Lee, W.C., et al., *Kinetics of transfemoral amputees with osseointegrated fixation performing common activities of daily living.* Clinical Biomechanics, 2007. **22**(6): p. 665-673. https://doi.org/10.1016/j.clinbiomech.2007.02.005
[5] Webster, J.B., et al., *Osseointegration research*, in *Full Stride*. 2017, Springer. p. 167-193. https://doi.org/10.1007/978-1-4939-7247-0_10

[6] Ward, D. and K. Robinson, *Osseointegration for the skeletal fixation of limb prostheses in amputations at the trans-femoral level.* The osseointegration book: From calvarium to calcaneus. Berlin (Germany): Quintessence, 2005: p. 463-76.
[7] Tomaszewski, P., et al., *A comparative finite-element analysis of bone failure and load transfer of osseointegrated prostheses fixations.* Annals of Biomedical Engineering, 2010. **38**(7): p. 2418-2427. https://doi.org/10.1007/s10439-010-9966-9
[8] Thesleff, A., B. Håkansson, and M. Ortiz-Catalan, *Biomechanical Characterisation of Bone-anchored Implant Systems for Amputation Limb Prostheses: A Systematic Review.* Annals of Biomedical Engineering, 2018. **46**(3): p. 377-391. https://doi.org/10.1007/s10439-017-1976-4
[9] Isaacson, B.M. and S. Jeyapalina, *Osseointegration: a review of the fundamentals for assuring cementless skeletal fixation.* Orthopedic Research and reviews, 2014. **6**: p. 55-65. https://doi.org/10.2147/ORR.S59274
[10] Frolke, J.P., R.A. Leijendekkers, and H. van de Meent, *Osseointegrated prosthesis for patients with an amputation : Multidisciplinary team approach in the Netherlands.* Unfallchirurg, 2017. **120**(4): p. 293-299. https://doi.org/10.1007/s00113-016-0302-1
[11] Tillander, J., et al., *Osseointegrated titanium implants for limb prostheses attachments: infectious complications.* Clinical Orthopaedics and Related Research®, 2010. **468**(10): p. 2781-2788. https://doi.org/10.1007/s11999-010-1370-0
[12] Brånemark, R., et al., *Osseointegration in skeletal reconstruction and rehabilitation: a review.* Journal of Rehabilitation Research and Development, 2001. **38**(2): p. 1-4.
[13] Morelli, F., et al., *Influence of bone marrow on osseointegration in long bones: an experimental study in sheep.* Clinical oral implants research, 2015. **26**(3): p. 300-306. https://doi.org/10.1111/clr.12487
[14] Sullivan, J., et al., *Rehabilitation of the trans-femoral amputee with an osseointegrated prosthesis: The United Kingdom experience.* Prosthetics and Orthotics International, 2003. **27**(2): p. 114-120. https://doi.org/10.1080/03093640308726667
[15] Cairns, N.J., et al., *Ability of modal analysis to detect osseointegration of implants in transfemoral amputees: a physical model study.* Medical Bbiological Engineering Computing, 2013. **51**(1-2): p. 39-47. https://doi.org/10.1007/s11517-012-0962-0
[16] Cairns, N.J., et al., *Evaluation of modal analysis techniques using physical models to detect osseointegration of implants in transfemoral amputees.* Conference proceedings : ... Annual International Conference of the IEEE Engineering in Medicine and Biology Society. IEEE Engineering in Medicine and Biology Society. Conference, 2011: p. 1600-1603. https://doi.org/10.1109/IEMBS.2011.6090463
[17] Vayron, R., et al., *Evaluation of dental implant stability in bone phantoms: Comparison between a quantitative ultrasound technique and resonance frequency analysis.* Clinical Implant Dentistry and Related Research, 2018. **20**(4): p. 470-478. https://doi.org/10.1111/cid.12622
[18] Chiu, W.K., et al., *Healing assessment of fractured femur treated with an intramedullary nail.* Structural Health Monitoring, 2019: p. 454. https://doi.org/10.1177/1475921718816781
[19] Vien, B.S., et al., *A Quantitative Approach for the Bone-implant Osseointegration Assessment Based on Ultrasonic Elastic Guided Waves.* Sensors, 2019. **19**(3). https://doi.org/10.3390/s19030454
[20] Isaacson, B.M., et al., *Effectiveness of resonance frequency in predicting orthopedic implant strength and stability in an in vitro osseointegration model.* Resonance, 2009. **37**(38): p. 43-60.
[21] Li, P., N. Jones, and P. Gregg, *Vibration analysis in the detection of total hip prosthetic loosening.* Medical Engineering & Physics, 1996. **18**(7): p. 596-600. https://doi.org/10.1016/1350-4533(96)00004-5

[22] Campoli, G., et al., *Relationship between the shape and density distribution of the femur and its natural frequencies of vibration.* Journal of biomechanics, 2014. **47**(13): p. 3334-3343. https://doi.org/10.1016/j.jbiomech.2014.08.008

[23] Lannocca, M., et al., *Intra-operative evaluation of cementless hip implant stability: a prototype device based on vibration analysis.* Medical Engineering & Physics, 2007. **29**(8): p. 886-894. https://doi.org/10.1016/j.medengphy.2006.09.011

[24] Varini, E., et al., *Assessment of implant stability of cementless hip prostheses through the frequency response function of the stem–bone system.* Sensors and Actuators A: Physical, 2010. **163**(2): p. 526-532. https://doi.org/10.1016/j.sna.2010.08.029

[25] Jaecques, S.V., C. Pastrav, and G. Van der Perre. *Analysis of the fixation quality of total hip replacements using a vibrational technique*. in *ASME 7th Biennial Conference on Engineering Systems Design and Analysis*. 2004. American Society of Mechanical Engineers. https://doi.org/10.1115/ESDA2004-58581

[26] Lu, S., et al., *Quantitative Monitoring of Osseointegrated Implant Stability Using Vibration Analysis.* Materials Research Proceedings. **18**.

[27] Xu, D., A. Crocombe, and W. Xu, *Numerical evaluation of bone remodelling associated with trans-femoral osseointegration implant–A 68 month follow-up study.* Journal of Biomechanics, 2016. **49**(3): p. 488-492. https://doi.org/10.1016/j.jbiomech.2015.12.028

[28] Rizzo, P., *A review on the latest advancements in the non-invasive evaluation/monitoring of dental and trans-femoral implants.* Biomedical Engineering Letters, 2020. **10**(1): p. 83-102. https://doi.org/10.1007/s13534-019-00126-8

[29] Lu, S., et al., *Experimental Investigation of Vibration Analysis on Implant Stability for a Novel Implant Design.* Sensors, 2022. **22**(4): p. 1685. https://doi.org/10.3390/s22041685

[30] Russ, M.V., AU), Chiu, Wingkong (Victoria, AU), Fitzgerald, Mark (Victoria, AU), *SURGICAL IMPLANT FOR SUPPORTING A PROSTHETIC DEVICE*. 2020, ALFRED HEALTH (Melbourne, Victoria, AU),MONASH UNIVERSITY (Clayton, Victoria, AU): United States.

[31] Russ, M., et al., *Development of a Novel Osseointegrated Endoprosthesis, Combing Orthopaedic and Engineering Design Principles, and Structural Health Monitoring Conc.* Structural Health Monitoring 2017, 2017(shm). https://doi.org/10.12783/shm2017/14244

[32] Chiu, W.K., et al., *Vibration-based healing assessment of an internally fixated femur.* Journal of Nondestructive Evaluation, Diagnostics and Prognostics of Engineering Systems, 2019. **2**(2): p. 021003. https://doi.org/10.1115/1.4043276

[33] Wade, R., C. Moorcroft, and P. Thomas, *Fracture stiffness as a guide to the management of tibial fractures.* Bone & Joint Journal, 2001. **83**(4): p. 533-535. https://doi.org/10.1302/0301-620X.83B4.0830533

[34] Claes, E.L. and L.J. Cunningham, *Monitoring the Mechanical Properties of Healing Bone.* Clinical Orthopaedics and Related Research, 2009. **467**(8): p. 1964-1971. https://doi.org/10.1007/s11999-009-0752-7

[35] Eriksson, C., et al., *Callus formation and remodeling at titanium implants.* Journal of Biomedical Materials Research Part A: An Official Journal of The Society for Biomaterials, The Japanese Society for Biomaterials, and The Australian Society for Biomaterials and the Korean Society for Biomaterials, 2007. **83**(4): p. 1062-1069. https://doi.org/10.1002/jbm.a.31433